Nafion−Montmorillonite Nanocomposite Membrane for the Effective Reduction of Fuel Crossover

Christine Felice, Stanley Ye,[†] and Deyang Qu*

Department of Chemistry, University of Massachusetts Boston, Boston, Massachusetts 01225

The effect of Nafion−clay nanocomposite membranes on hydrogen and methanol crossover in a proton exchange membrane (PEM) fuel cell was studied. Several analytical methods were used to determine the fuel crossover rate and the ionic conductivity of the membranes. It is the first time a Nafion−clay nanocomposite was investigated to reduce the hydrogen migration rate across the PEM membrane. The Nafion−clay nanocomposites demonstrated significantly reduced permeability to both methanol and hydrogen. The reduction of hydrogen and methanol crossover was compared, and the possible mechanistic difference was discussed. The ionic conductivities for both in-plane and through-plane were measured using alternating current impedance techniques. The ionic conductivities of the Nafion−clay nanocomposites were lower than a pure Nafion membrane of the same thickness.

I. Introduction

The history of proton exchange membrane (PEM) fuel cell evolution is in parallel with the development of the membranes. The first PEM fuel cell served as the power plant for the Gemini space mission in the early 1960s. Developed by GE using polystyrene sulfonic acid polymer, these fuel cells were not durable due to their low resistance to an oxidative environment. The milestone was the invention of the fluorocarbon sulfonic acid polymer with the trade name Nafion by DuPont, which was subsequently adopted by GE to meet its commitment to the NASA space program.[1] Nafion is now widely used as a PEM in both H_2 fuel cells and direct methanol fuel cells (DMFC).

In 1989, Toyota started to use a nylon−clay nanocomposite in its vehicles, substantially increasing tensile strength. Since then, polymer−clay nanocomposites have attracted significant attention as a new and important category of polymeric composites, providing a new avenue for the significant enhancement of mechanical and barrier properties.[2,3]

Clay minerals are a class of compounds with a layered structure. For example, the most widely used clay, montmorillonite (MMT), has an ideal chemical formula of $Al_2Si_4O_{10}(OH)_2 \cdot yH_2O$ and is a layered silicate composed of silica tetrahedral and alumina octahedral sheets. In most cases, the alumino-silicate sheets are stacked by van der Waals forces. The interlayer space is in the range of a nanometer. The guest species, normally cations, are trapped in the interlayer spaces. Such guest species can be replaced by ionic exchange or the intercalation of a host polymer molecule. When organic species enter the silicate interlayer, the interlayer space will expand and eventually could be exfoliated. The degree of interlayer expansion caused by the host polymer depends not only on the intrinsic properties of the clay and polymer but also on the preparation conditions. After the addition of clay, the properties of polymers could largely be improved due to the formation of a nanocomposite. The resulting polymer−clay nanocomposites could offer substantial increases in tensile strength and significant improvements in barrier properties against the permeation of gas, solvent, and moisture. For example, the permeation coefficient of water vapor for polyimides used for microelectronics was reduced by 54% with only the addition of 2 wt % montmorillonite;[4] oxygen permeability of the biodegradable polymer PLA was decreased by 35% after forming a nanocomposite with 4 wt % organically modified mica.[5] Even though the detailed mechanism for such enhancement in barrier properties was not fully understood, Nielson's tortuous path model[6,7] was widely used to explain the phenomenon with the presence of clay in polymer. The key parameters that impact the permeability are the dispersed-phase volume fraction of impermeable fillers, the particle aspect ratio, and the orientation of the clay platelets. The latter parameter explains the effectiveness of the clay layers in building a barrier to the permeating gas molecules. The hypothesis was that nanosized clay platelets create a maze, or "tortuous path", that retards the progress of the gas molecules through the polymer matrix.

Polymer−clay nanocomposites were reported to reduce the methanol permeability in direct methanol fuel cells.[8−10] The major obstacle for the commercialization of DMFCs is the methanol crossover, which becomes substantial at a high methanol concentration. When it happens, the methanol reacts at the cathode without producing electricity. This will not only reduce the fuel utilization but also decrease the catalyst activity at the cathode. A polymer−clay nanocomposite could reduce the methanol migration rate across the PEM membrane. It is the first time, however, hydrogen crossover was investigated. Even though the small amount of hydrogen that permeates through the membrane generates heat and water, leading to a fuel inefficiency, hydrogen crossover is less of a problem when a fuel cell operates under near-ambient conditions than under the high-pressure conditions, e.g. 3000 psi. In this report, Nafion−montmorillonite nanocomposite membranes were synthesized to reduce fuel crossover while maintaining high proton conductivity, which is essential for fuel cell operation.

II. Experimental Details

2.1. Material. Nafion dispersion was purchased from IonPower, New Castle, DE. Five percent of acid-form Nafion was dispersed in an isopropyl alcohol water solution. Nafion membranes 115, 211, and 212 were also purchased from IonPower. *N*-Methylpyrolidinone (NMP) and *N*,*N*′-dimethylaceta-

* To whom correspondence should be addressed. E-mail: deyang.qu@umb.edu. Tel.: 617-287-6035. Fax: 617-287-6188.

[†] Summer Intern, undergraduate student of Department of Chemistry, Brandeis University.

10.1021/ie901600a
Published on Web 01/07/2010

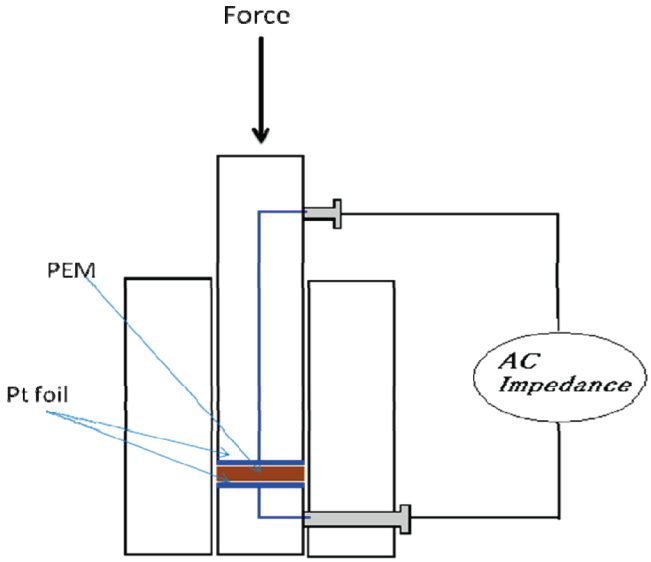

Figure 1. Conductivity cell used for two-probe through-plane conductivity measurements. The cell body was made with Teflon, and a current contactor was made with Pt foil. The cell was put under a vertical hand wheel test stand (IMADA model HV-110S) equipped with a digital force gauge (IMADA model DS2). The conductivity was measured using alternating current (AC) impedance technique.

mide (DMA) were purchased from Sigma-Aldrich. Montmorillonite (MMT) was provided from Southern Clay Product, Inc., Austin, TX. All chemicals were used without further purification or treatments.

2.2. Preparation of Nafion−MMT Nanocomposite Membranes. There are three common methods for the preparation of polymer−clay nanocomposites. They are in situ polymerization, solution methods, and melt-processing methods. The solution methods were chosen for this investigation.

NMP and DMA were first mixed at 1:9 weight ratio. The NMP/DMA solution was then added to a 5% Nafion dispersion. The mixture was mechanically mixed thoroughly to form a homogeneous dispersion. Then the dispersion was condensed in a fume hood overnight. Most of the isopropyl alcohol evaporated and was replaced with high boiling point NMP and DMA. A 40% weight loss was observed for the solution. The viscous dispersion was then mixed with MMT at the desired weight ratio. The mixture was then either sonicated or vigorously mixed mechanically. The resulting paste was then cast on a glass plate using a doctor blade, forming Nafion−clay membranes at various thicknesses.

After curing at 120 °C for 10 h, the casted membrane was soaked in 80 °C DI water for 5 h. The Nafion−clay membranes were then kept in Ziploc bags. Before measurements were conducted, the Nafion−clay was soaked in DI water at 80 °C overnight to ensure full hydration.

2.3. Conductivity Measurements. A four-probe Teflon conductivity cell was purchased from BekkTech LLC. The cell is designed for the measurement of in-plane membrane conductivity. Four Pt wires were used as electrodes. The Nafion membrane was sandwiched between two Teflon grates and the Pt electrodes were forced against the membrane.

Figure 1 shows the homemade two-probe Teflon conductivity cell, which is designed to measure the through-plane membrane conductivity. Two Pt disks were used as contacts, and the Nafion membrane resided between the two Pt disks. Adjustable forces can be imposed on the cell in order to investigate the impact of contact resistance between the Pt electrodes and membrane.

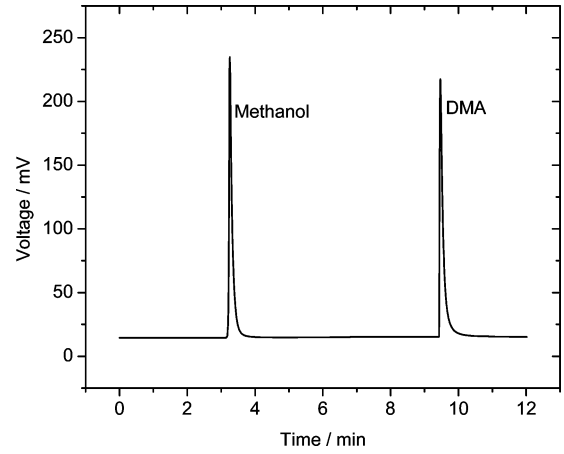

Figure 2. Typical GC-FID profile for methanol and DMA.

AC impedance was used to measure the conductivity. The true ohmic resistance was measured by taking the real impedance at the point that the imaginary impedance was equal to zero or when the phase angle was zero.

All measurements were conducted under ambient conditions with temperature at 18 ± 1 °C and relative humidity (RH%) at 33 ± 5%.

2.4. Instrumental Details. All of the electrochemical measurements, including limiting current and conductivity measurements, were carried out using a Solarton (SI 1287). A ChemInstrument EZ Coater (EC100) modified in-house with a doctor-blade attachment was used for membrane coating. A vertical hand wheel test stand (IMADA model HV-110S) equipped with a digital force gauge (IMADA model DS2) was used to apply force on the conductive cell. An Agilent gas chromatograph equipped with a flame ionization detector (GC-FID) was used to analyze the concentration of methanol. DMA was used as the internal standard. Nitrogen was used as the carrier gas.

2.5. Methanol and Hydrogen Crossover Measurements.

2.5.1. Methanol Crossover Measurement. A two-compartment cell was made to facilitate the measurement of methanol crossover during storage. The cell is composed of two connected compartments with one filled with 30% methanol and the other with DI water. The samples were taken at various times from the compartment with DI water, and the concentration of methanol was analyzed with GC-FID and NMR. The volume of sample taken from the cell was substantially small compared to the volume of the cell. Figure 2 shows a typical GC diagram for the analysis. The percentage of methanol was determined from the ratio of the methanol peak area and DMA peak area.

2.5.1. Hydrogen Crossover Measurement.[11,12] The device for the in situ measurement for hydrogen crossover is shown in Figure 3. An H^+/H_2 reference electrode is implanted on the graphite H_2 flow plate by connecting a Pt wire to a small piece of a Pt-loaded catalyst layer, which is isolated from the gas diffusion electrode. The reference electrode enables the real-time diagnostic analysis for the cell stack during the fuel cell operation. The electrochemical measurement of gas permeation is used to determine the hydrogen permeation rate. The method is to measure the mass-transfer limiting current, which is proportional to the concentration of hydrogen. Ultrapure hydrogen flowed through the compartment housing the counter electrode and reference electrode. The hydrogen pressure was held at 30 psig. The compartment where the working electrode resided was maintained at the same gas pressure by flowing ultrapure nitrogen gas through it. The monitoring technique

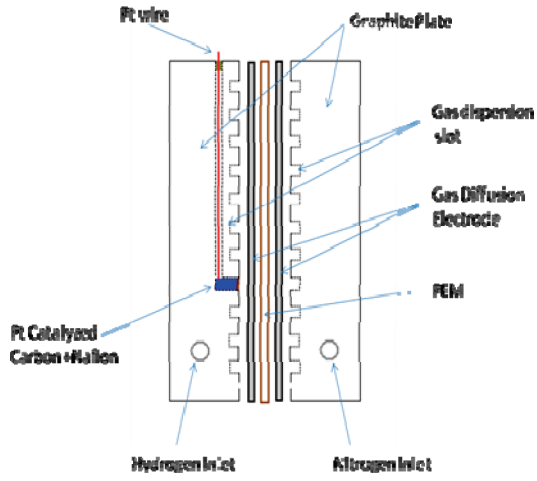

Figure 3. Schematic of the fuel cell fixture used for hydrogen permeation tests. The gas diffusion electrode with Pt catalyst was used for the electrodes.

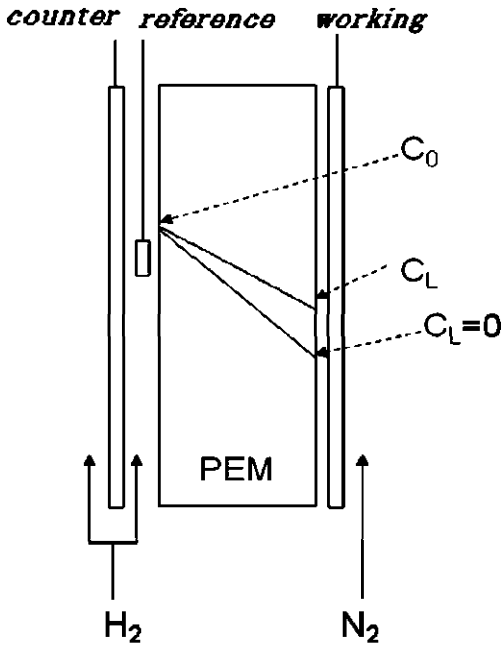

Figure 4. Schematic of the in situ electrochemical measurement for limiting current. The compartment with reference electrode was filled with 30 psig ultrapure H_2 and another compartment was filled with 30 psig ultrapure N_2. Linear sweep potential was applied against H^+/H_2 reference electrode. The H_2 concentration gradient inside the PEM is assumed to be linear. The limiting current is reached when $C_L = 0$.

consisted of measuring the limiting current generated as all the hydrogen molecules permeating through the membrane became oxidized under mass-transfer limiting conditions.

III. Results and Discussion

3.1. Fuel Crossover. The crossover current is linearly proportional to the partial pressure of hydrogen in the hydrogen chamber; the permeability coefficient of the membrane is inversely proportional to the thickness of the membrane. Thus, the hydrogen permeation from anode to cathode could not be ignored if the fuel cell operates at high-pressure conditions. The hydrogen that migrates into the cathode side could be either recombined with oxygen chemically or electrochemically oxidized with high overpotential of hydrogen reaction at the cathode. Either way, the fuel is consumed without generating energy.[11] That amount of H_2, instead of generating electric

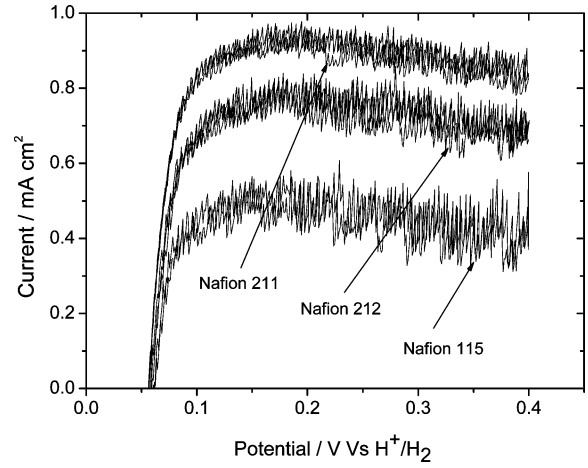

Figure 5. Linear voltammetry for Nafion 211, 212, and 115. The sweep rate was 0.1 mV s^{-1}. Replicate curves are plotted to demonstrate the reproducibility.

energy, will produce heat. Under high-pressure conditions, a substantial amount of H_2 would permeate through the PEM membrane and significantly deplete the fuel cell efficiency. Thus, the H_2 crossover has significant negative impact for the low discharge rate applications under high hydrogen partial pressure. Development of the PEM membrane with low H_2 permeation becomes critical for those applications.

Among many other alternative techniques for the measurement of gas permeation, by monitoring the change of mass-transfer limiting current, the in situ electrochemical measurement is the most direct, flexible method. By means of the technique, the gas permeation rate can be monitored real-time inside a fuel cell while it operates. Figure 4 shows how the measurement works schematically. Hydrogen was maintained at a fixed pressure (30 psig) on the side of the fuel cell where the reference electrode resides, while nitrogen was maintained at the same pressure in the other side of the PEM membrane. The flow rates for both hydrogen and nitrogen were kept low, so the PEM membrane did not dry during the duration of the measurement. The hydrogen molecules that crossed over to the other side of the membrane got oxidized at the carbon electrode loaded with Pt catalyst. When the applied potential is high enough that all hydrogen molecules become oxidized as soon as they reach the electrode, the oxidation current reaches its maximum due to the mass-transfer limitation. The mass-transfer limiting current is proportional to the hydrogen permeation rate assuming the hydrogen concentration gradient within the PEM membrane is linear, as shown in Figure 4. The relation between the limiting current, H_2 diffusion coefficient and permeability coefficient can be derived as shown in the Appendix.

$$\text{diffusion coefficient: } D_i = \frac{I_{max} RTL}{nFP} \tag{1}$$

$$\text{permeability coefficient: } k_i = \frac{\text{rate} \times L}{\Delta P_i} = \frac{I_{max} L}{nFP} \tag{2}$$

Both the diffusion coefficient and permeability coefficient for H_2 crossover can be determined by measuring the limiting current of H_2 oxidation under certain H_2 partial pressures.

Figure 5 shows the linear voltammetry for the various commercially available PEM membranes. Nafion membranes 211, 212, and 115 represent the membranes made with 1100 E.W. Nafion with thicknesses of about 1, 2, and 5 mil, respectively. Three repetitions were done for each membrane,

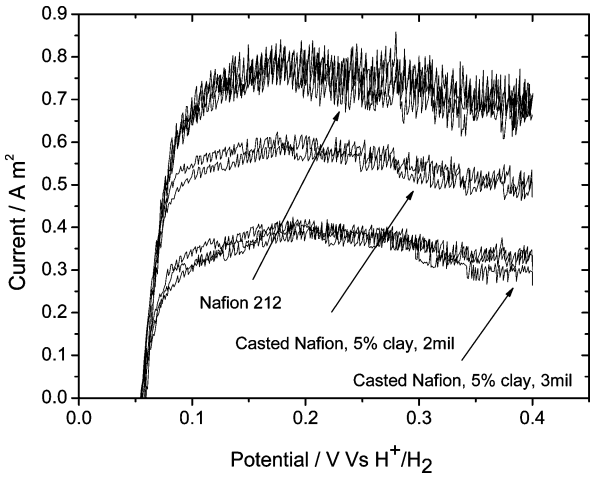

Figure 6. Comparison of linear voltammetry for Nafion 212 and Nafion−clay nanocomposite membranes with 5% clay. The dry thickness for the nanocomposite membranes were 2 and 3 mil, respectively.

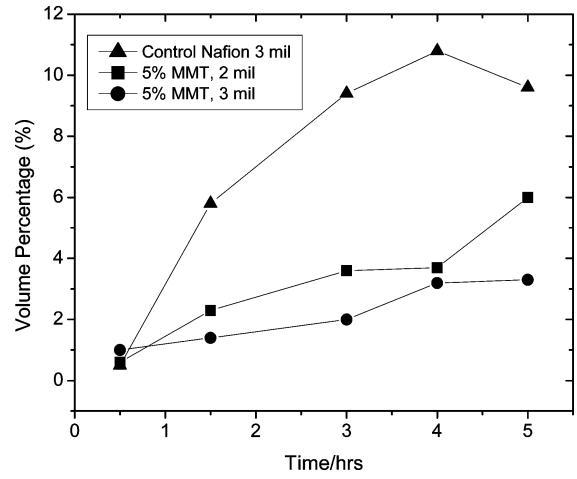

Figure 7. Comparison of methanol crossover for the 3 mil of control Nafion and Nafion−clay nanocomposite membranes with 5% MMT. The dry thicknesses of the nanocomposite membranes were 2 and 3 mil, respectively.

Table 1. H_2 Crossover Characteristics of Various Membranes (NC, Nafion−MMT Nanocomposite Membrane)

membrane	I_{max} (A m^{-2})	thickness (m × 10^{-5})	D (m^2 s^{-1} × 10^{-11})	K(mol m^{-1} s^{-1} Pa^{-1} × 10^{-15})	conductivity (mS cm^{-1})
211	9.1	2.54	0.96	3.89	15.57
212	7.7	5.08	1.62	6.58	13.47
115	5.2	12.7	2.73	11.1	11.5
5% NC	5.4	5.08	1.13	4.61	1.68
5% NC	3.1	7.62	0.98	3.97	4.03

and the results are all plotted in Figure 5. The experiments are proven to be very reproducible. The limiting current is clearly demonstrated for all three membranes. It appears that the thicker the membrane, the lower the H_2 crossover rate. The slight decrease of the limiting current as the potential scans to more positive potential is a common phenomenon for almost all the membranes tested in the investigation. The cause of the decrease is unclear. But the decrease did not result from moisture loss, since the multiple potential dynamic scans on the same membrane were very reproducible as shown in Figure 5. Figure 6 shows the comparison of linear voltammetry for the Nafion−MMT nanocomposite membranes loaded with 5% clay and Nafion 212. The thicknesses of the composite membranes were 2 and 3 mil. Again, a limiting current can be observed. The impact of clay on the reduction of H_2 permeation is clearly demonstrated. The diffusion coefficient and permeability coefficient were also calculated using eqs 1 and 2. The results are tabulated in Table 1. Obviously, the H_2 permeation rate was significantly reduced by using a Nafion−MMT nanocomposite.

Figure 7 shows the methanol crossover in the initial 5 h. Nafion−MMT nanocomposites demonstrated almost 50% reduction of methanol crossover. After 24 h, the methanol concentration in the compartments on both sides of the Nafion membrane were almost the same (15 vol %). However, if a Nafion−MMT nanocomposite was used as the separator, the methanol concentration on the side which contained DI water initially was about 10 vol %. The methanol permeation rate was also significantly reduced by using a Nafion−MMT nanocomposite.

As shown in Figures 6 and 7, the Nafion−MMT nanocomposite demonstrated the potential of significant reduction of H_2 and methanol permeation, respectively. Figure 8 illustrates the hypothesis for the fuel permeation through the Nafion−MMT nanocomposite. Rather than directly passing through, the diffusion path of penetrating mass is significantly altered and becomes a "tortuous path". Not only is the diffusion length

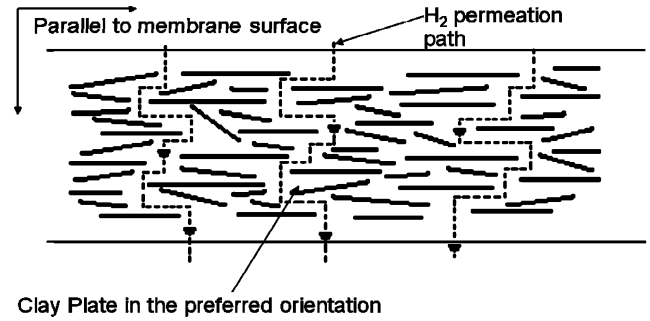

Figure 8. Hypothesis of the preferred orientation of the clay platelets in the Nafion and the impact on H_2 crossover.

substantially increased, but the diffusion rate is reduced as well. Thus, the mass permeation rate could be significantly reduced. After investigating the hydrogen diffusion coefficients and solubilities of hydrogen in both aqueous and fluorocarbon phases, it is likely that hydrogen molecules diffuse through the interfacial area between the aqueous phase and the hydrophobic fluorocarbon phase,[12] or the permeation of hydrogen takes place in the intermediate region of the flexible amorphous part of perfluorocarbon backbone of Nafion.[13] But it seems the substantial portion of the "interfacial area" is in the aqueous phase.[12] It is interesting to note from Table 1 that the diffusion coefficients of the commercially available Nafion membranes 211, 212, and 115 were not the same. Ideally, the H_2 diffusion coefficient for pure Nafion should not change with the thickness. The phenomenon could be related to the inherent structural anisotropy of the backbone matrix for the commercial membrane made by an extrusion process.[14] The extrusion manufacturing process could lead to a preferred orientation of the ionomer backbone, which is related to the draw speed of the extrusion. Such orientation could be further enhanced during the membrane electrode assembling process, e.g., uniaxial stretching of the Nafion membranes. For the nanocomposite membrane, of course the nonuniform orientation of the clay would also have impact on the diffusion coefficients. Further investigation to understand the deficiency is in progress. It is worthwhile to point out that the impact of membrane thickness was less substantial for methanol diffusion. It appears that the methanol crossover rate for 2 and 3 mil Nafion−MMT nanocomposites were not as different as that of H_2 permeation. Such difference could result from the different migration mechanism for hydrogen and

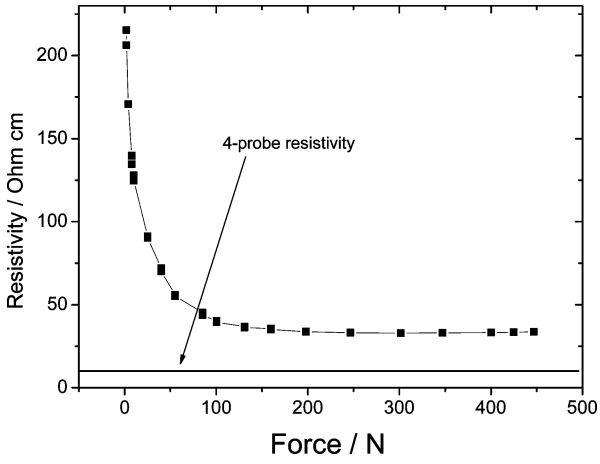

Figure 9. Typical change of the two-probe through-plane resistivity with increasing stacking pressure. The resistivity measured with the four-probe technique is also included as reference.

methanol. If the hydrogen molecules diffuse through the "interfacial area", the diffusion of methanol could happen within the aqueous phase inside the pores of Nafion, even though the blocking mechanism for the clay could be the same.

3.2. Ionic Conductivity. The barrier properties of polymers to hydrogen permeation can be significantly altered by inclusion of clay platelets with sufficient aspect ratios to change the diffusion path of hydrogen molecules, as shown in Figure 8. To take full advantage of the barrier properties of clay platelets and maximize their capability of blocking the migration of hydrogen molecules, the platelets must be orientated perpendicular to the hydrogen permeation path, as shown in the figure. Such preferred orientation is promoted by the 2D layer structure of the clay nanoparticles, which tend to align parallel to the surface of the membrane under the shear force. Thus the alignment of platelets is affected by the membrane casting procedure. The preferred orientation of the clay platelets may result in the anisotropic conductivity of the Nafion−MMT nanocomposite. The four-probe tangential direction conductivity, which can minimize the interfacial contact resistance between the metal probes and membrane, cannot resemble the proton conduction direction through the membrane during the practical fuel cell operation. Thus, the information for the through-plane conductivity is closer to the real fuel cell operation. The homemade two-probe conductivity cell as shown in Figure 1 was used to measure the conductivity perpendicular to the membrane surface. The major challenge for such a measurement is to minimize the contact resistance between the Pt electrode and the membrane. To solve the problem, a series of conductivities were measured under various stacking pressures. Figure 9 shows the resistivity change during the increase of stacking pressure. The resistivity decreased with the pressure initially and eventually flatted out. The conductivity measured using the four-probe method is also shown in the figure as reference. It appears the contact resistance becomes insignificant over 150 N; the protonic conductivity contributed the majority of the total conductivity. However, the through-plane resistivity was still higher than that of the in-plane conductivity measured by means of the four-probe method. It seems the resistivity of the Nafion−MMT nanocomposite is anisotropic and the in-plane conductivity is higher than the through-plane conductivity. Figure 10 shows the relationship of the in-plane vs through-plane conductivities of the membranes synthesized under various conditions. It is worth emphasizing that the hypothesis of anisotropic resistivity is based on the model for the morphology

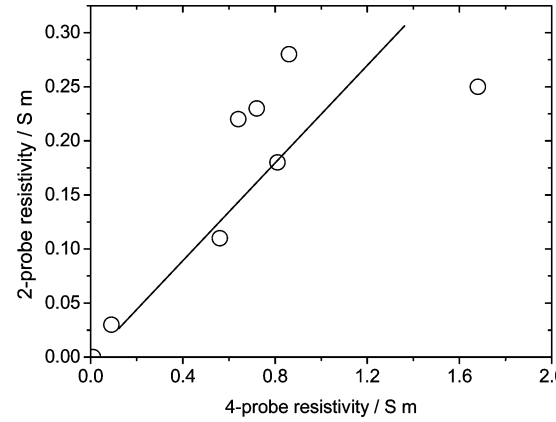

Figure 10. Relationship between the through-plane conductivities and four-probe conductivities.

of Nafion−MMT membranes as shown in Figure 8. It is feasible, at least theoretically, to differentiate the contact resistance from the total resistance by numerical fitting of AC impedance. The investigation is in progress and will be reported later. Nevertheless, the through-plane resistance is more critical to the fuel cell performance than in-plane resistance since that is the direction for proton diffusion during normal operation.

Nafion membranes consist of distinctive regions of a hydrophobic fluorocarbon backbone, hydrophilic sulfonate groups, and the water of hydration. The protonic conductivity relies on the arrangement of the polymer chains in the membrane, while the process of membrane formation and the composition of the membrane have significant impact on the structure of the membrane. The short-range interactions between the hydrophobic perfluorinated backbones and the hydrophilic sulfonate groups and long-range static interaction between the electrostatic charges all play important roles in forming the protonic conduction network. The proton diffusion could be through two pathways: one is due to proton migration in the aqueous phase, and another is due to the proton tunneling between adjacent sulfonate groups in narrow pores.[14,15] In a Nafion−MMT nanocomposite membrane, as shown in Figure 8, along with the preferential orientation of exfoliated clay plates, the hydrophobic backbones could align in the uniaxial direction. Thus, the random orientation of perfluorinated polymer backbones in the casted isotropic membrane changes to the preferred orientation of the ionomer backbone in a Nafion−MMT nanocomposite membrane, which is morphologically similar to the anisotropy in extruded commercial ionomeric membranes. Such morphology would make conductivity anisotropic for Nafion−MMT nanocomposites.

The observed conductivities of the membranes in the experiment were lower than typically reported for Nafion membranes. The measurements were carried out at ambient relative humidity, which is about 33%. Nafion membranes exhibit the best conductivity at a high relative humidity (>90%). The hydration of the membrane is essential for proton conductivity because the water molecules enhance the protonic conduction network of the membrane.

Fuel crossover decreases the efficiency of a fuel cell. Reducing this crossover will help improve a cell's performance. The nanocomposite membranes we studied are less conductive than the commercial Nafion membranes, but the benefit from a reduction of fuel crossover will outweigh this if the fuel cell is discharged at a low rate. The decrease in conductivity is less important for the low-rate application.

IV. Conclusion

Investigation of the conductivity of and fuel crossover through Nafion−MMT nanocomposite membranes has revealed that the permeation of fuel can be substantially reduced by using Nafion−MMT nanocomposites. Both the addition of clay to the membrane and the thickness of the nanocomposite membrane play important roles.

The addition of clay to the Nafion membranes reduces both the hydrogen and methanol crossover when compared to a control membrane of the same thickness. The thicker nanocomposite membrane also reduces the fuel crossover, though methanol crossover is less sensitive to the thickness. The dependence of the diffusion coefficient on the thickness of the membrane results from the inherent structural anisotropy of the backbone matrix and nonuniform clay orientation.

V. Appendix

where D is the diffusion coefficient. Assuming a linear

$$\text{rate} = -D_i\left(\frac{\partial C_i}{\partial x}\right)_t$$

concentration gradient,

$$\text{rate} = -D_i\left(\frac{C_H - C_N}{L}\right)$$

where L is the thickness of the membrane and C is the concentration of H_2 at hydrogen and nitrogen sides.

$$I = nF(-\text{rate})$$
$$= nFD_i\left(\frac{\partial C_i}{\partial x}\right)_t = nFD_i\left(\frac{C_i - C_o}{L}\right)$$

When the limiting current is reached,

$$C_N = 0; \quad \text{thus, } I_{max} = nFD_i\left(\frac{C_H}{L}\right)$$

$$PV = nRT; \quad \text{then } C_H = \frac{n}{V} = \frac{P}{RT}$$

$$I_{max} = \frac{nFD_iP}{RTL}$$

Diffusion coefficient:

$$D_i = \frac{I_{max}RTL}{nFP} \tag{1}$$

Permeability coefficient:

$$k_i = \frac{\text{rate} \times L}{\Delta P_i} = \frac{I_{max}L}{nFP} \tag{2}$$

Acknowledgment

The work was partially supported by the National Aeronautics and Space Administration through a subcontract and partially supported through the UMB new faculty start-up grant. The financial support of both is gratefully acknowledged. We also thank Professor Bela Torok, UMass Boston and his graduate student Mr. Dmitry Borkin for their support.

Literature Cited

(1) Banerjee, S.; Curtin, D. E. Nafion ® perfluorinated membranes in fuel cells. *J. Fluorine Chem.* **2004**, *125*, 1211.

(2) Chen, B.; Evans, J. R. G.; Greenwell, H. C.; Boulet, P.; Coveney, P. V.; Bowden, A. A.; Whiting, A. A critical appraisal of polymer-clay nanocomposites. *Chem. Soc. Rev.* **2008**, *37*, 568.

(3) Casciola, M.; Capitani, D.; Comite, A.; Donnadio, A.; Frittella, V.; Pica, M.; Sganappa, M.; Varzi, A. Nafion-zirconium phosphate nanocomposite membranes with high filler lodadings: Conductivity and mechanical properties. *Fuel Cells* **2008**, *8*, 217.

(4) Yano, K.; Usuki, A.; Okada, A.; Kurauchi, T.; Kamigaito, O. Synthesis and properties of polyimide-clay hybrid. *J. Polym. Sci., Part A: Polym. Chem.* **1993**, *31*, 2493.

(5) Ray, S. S.; Yamada, K.; Okamoto, M.; Gujimoto, Y.; Ogami, A.; Ueda, K. New polylactide/layered silicate nanocomposites. 3. High-performance biodegradable materials. *Chem. Mater.* **2003**, *15*, 1456.

(6) Nielsen, L. E. Models for the permeability of filled polymer systems. *J. Macromol. Sci. Chem. A* **1967**, *1*, 929.

(7) Bharadwaj, R. K. Modeling the barrier properties of polymer-layered silicate nanocomposites. *Macromolecules* **2001**, *34*, 9189.

(8) Song, M. K.; Park, S. B.; Kim, Y. T.; Kim, K. H.; Min, S. K.; Rhee, H. W. Characterization of polymer-layered silicate nanocomposite membranes for direct methanol fuel cells. *Electrochim. Acta* **2004**, *50*, 639.

(9) Kim, D. W.; Choi, H. S.; Lee, C.; Blumstein, A.; Kang, Y. Investigation on methanol permeability of Nafion modified by self-assembled clay-nanocomposite multilayers. *Electrochim. Acta* **2004**, *50*, 659.

(10) Choi, Y. S.; Kim, T. K.; Kim, E. A.; Joo, S. H.; Pak, C.; Lee, Y. H.; Chang, H.; Seung, D. Exfoliated sulfonated poly(arylene ether sulfone)-clay nanocomposites. *Adv. Mater.* **2008**, *20*, 2341.

(11) Kocha, S. S.; Yang, J. D.; Yi, J. S. Characterization of gas crossover and its implications in PEM fuel cells. *AIChE* **2006**, *52*, 1916.

(12) Tsou, Y. M.; Kimble, M. C.; White, R. E. Hydrogen diffusion, solubility, and water uptake in Dow's short-side-chain perfluorocarbon membranes. *J. Electrochem. Soc.* **1992**, *139*, 1913.

(13) Ogumi, Z.; Kuroe, T.; Takehara, Z. Gas permeation in SPE method. *J. Electrochem. Soc.* **1985**, *132*, 2601.

(14) Allahyarov, E.; Taylor, P. L. Simulation study of the correlation between structure and conductivity in stretched Nafion. *J. Phys. Chem. B* **2009**, *113*, 610.

(15) Tsampas, M. N.; Pikos, A.; Brosda, S.; Katsaounis, A.; Vayenas, C. G. The effect of membrane thickness on the conductivity of Nafion. *Electrochim. Acta* **2006**, *51*, 2743.

Received for review October 13, 2009
Revised manuscript received December 11, 2009
Accepted December 15, 2009

IE901600A